

# Comparative study of auxetic geometries by means of computer-aided design and engineering

Q.1 **Juan Carlos Álvarez Elipe and Andrés Díaz Lantada**

Mechanical Engineering Department, Universidad Politécnica de Madrid, c/ José Gutiérrez Abascal 2, 28006 Madrid, Spain

E-mail: [adiaz@etsii.upm.es](mailto:adiaz@etsii.upm.es)

Received 16 April 2012, in final form 27 June 2012

Published

Online at [stacks.iop.org/SMS/21/000000](http://stacks.iop.org/SMS/21/000000)

(Ed: Lauret)

Ascii/Word/SMS/

sms429872/PAP

Printed 19/7/2012

Spelling US

Issue no

Total pages

First page

Last page

File name

Date req

Artnum

Cover date

## Abstract

Auxetic materials (or metamaterials) are those with a negative Poisson ratio (NPR) and display the unexpected property of lateral expansion when stretched, as well as an equal and opposing densification when compressed. Such geometries are being progressively employed in the development of novel products, especially in the fields of intelligent expandable actuators, shape morphing structures and minimally invasive implantable devices. Although several auxetic and potentially auxetic geometries have been summarized in previous reviews and research, precise information regarding relevant properties for design tasks is not always provided.

In this study we present a comparative study of two-dimensional and three-dimensional auxetic geometries carried out by means of computer-aided design and engineering tools (from now on CAD–CAE). The first part of the study is focused on the development of a CAD library of auxetics. Once the library is developed we simulate the behavior of the different auxetic geometries and elaborate a systematic comparison, considering relevant properties of these geometries, such as Poisson ratio(s), maximum volume or area reductions attainable and equivalent Young's modulus, hoping it may provide useful information for future designs of devices based on these interesting structures.

## 1. Introduction

When a material is stretched there is normally an accompanying reduction in width. A measure of this dimensional change can be defined by the Poisson ratio,  $\nu = -d\varepsilon_{\text{trans}}/d\varepsilon_{\text{axial}}$ ,  $\varepsilon_{\text{trans}}$  and  $\varepsilon_{\text{axial}}$  being the transverse and axial strains when the material is stretched or compressed in the axial direction. In a more general case,  $\nu_{ij}$  is the Poisson ratio that corresponds to a contraction in direction 'j' when an extension is applied in direction 'i'. For most materials this value is positive and reflects a need to conserve volume. Auxetic materials (or metamaterials) are those with a negative Poisson ratio (NPR) and display the unexpected property of lateral expansion when stretched, as well as an equal and opposing densification when compressed [1–4]. Natural (some minerals, skins, ...) and man-made (foams,

Gore-Tex®, polymeric foams) auxetics have been described and very special attention is being paid to the development of auxetic structures designed and controlled on a molecular scale [5].

Auxetic geometries are being progressively employed in the development of novel products, especially in the fields of intelligent expandable actuators, shape morphing structures and minimally invasive implantable devices. Regarding smart actuators based on an auxetic structure, it is important to cite some recent progress linked to auxetic shape-memory alloys (SMA) for developing deployable satellite antennas [6] and some research on the characterization of polyurethane foams with shape-memory behavior and auxetic properties, promoted thanks to several post-processing stages [7]. In the area of medical devices, recent research has also assessed the behavior of a few auxetic geometries for

Q.2

implementing expandable stents [8] and their application to other implantable biodevices is clearly a matter of research.

Several auxetic and potentially auxetic geometries, normally grouped under the terms ‘re-entrant’, ‘chiral’ and ‘rotating’ in relation to the characteristics that promote the auxetic behavior, have been summarized in previous reviews and research. However, precise information regarding the values of Poisson ratios is not always provided, due to difficulties with simulating and manufacturing such complex geometries. Sometimes just a scheme of their folding process, when submitted to uniaxial stresses, is provided, which proves to be limited for subsequent design activities. Additional information of relevant properties of different auxetic geometries, methodically compared, would therefore be beneficial for material–structure selection tasks for the development of novel foldable–morphing actuators, structures and devices.

In this study we present a comparative study of two-dimensional and three-dimensional auxetic geometries carried out by means of computer-aided design and engineering tools. The first part of the research exposed is focused on the development of a CAD library of auxetic and potentially auxetic geometries–structures, including seven three-dimensional structures and 25 two-dimensional structures, based on or adapted from the information included in previous review publications, conference proceedings and patents, as well as some we have developed ourselves. Once the library is developed we simulate the behavior of the different auxetic geometries and elaborate a systematic comparison, considering relevant properties of these geometries for the development of actuators and morphing structures, such as Poisson ratio(s), maximum volume or area reductions attainable, equivalent Young’s modulus and density.

Such properties are defined as follows.

- Poisson ratios:  $\nu_{zx} = -\Delta x/\Delta z$  and  $\nu_{zy} = -\Delta y/\Delta z$ , ‘z’ (vertical axis) being the direction of axial compression used further on and  $\Delta x$ ,  $\Delta y$ ,  $\Delta z$  the displacements obtained.
- Maximum volume/area reduction:  $MVR = -(V_0 - V_f)/V_0$  and  $MAR = -(A_0 - A_f)/A_0$ .  $V_0$  and  $A_0$  are respectively the values of the initial volumes of the 3D auxetics and areas of the planar auxetics.  $V_f$  and  $A_f$  are the final volumes and areas of the auxetics, after application of the uniaxial loading levels that lead to the beginning of contacts between inner features, thus also promoting the beginning of buckling and structure collapse.
- Equivalent Young’s modulus:  $E_{z, \text{auxetic}} = E_{z, \text{eq}} = \sigma_{z, \text{eq}}/\varepsilon_{z, \text{eq}} = [\Sigma F_z/(ab)]/[-\Delta z/c]$ ,  $\Sigma F_z$  being the total compressive force applied in the simulations (along the z axis) and  $a$ ,  $b$ ,  $c$  the global dimensions of the different structures under study measured along axes  $x$ ,  $y$ ,  $z$ .
- Equivalent density:  $\rho_{\text{auxetic}} = \rho_{\text{eq}} = \rho_{\text{bulk}}[V_{\text{auxetic}}/(abc)]$ ,  $\rho_{\text{bulk}}$  being the density of the bulk material,  $V_{\text{auxetic}}$  the volume of the planar or three-dimensional auxetic structure (measured with the help of a computer-aided design program) and again  $a$ ,  $b$ ,  $c$  the global dimensions of the different structures under study, measured along axes

$x$ ,  $y$ ,  $z$ . Such a definition is valid for three-dimensional and planar auxetics as in the case of a planar auxetic the expression would lead to:  $\rho_{2D, \text{auxetic}} = \rho_{\text{bulk}}[V_{\text{auxetic}}/(abc)] = \rho_{\text{bulk}}[(A_{\text{auxetic}} \text{dota})/(abc)] = \rho_{\text{bulk}}[(A_{\text{auxetic}})/(bc)]$ ,  $A_{\text{auxetic}}$  being the area of the planar auxetic measured in plane  $ZY$ .

To our knowledge, the present study constitutes one of the most comprehensive comparative studies of auxetic geometries realized to date, providing a blind validation for several prior studies, complementing some of the references with additional data and helping to detect various problems with a few geometries, typically described as ‘potentially auxetic’ in several references and websites, but whose auxetic behavior is actually prevented due to buckling phenomena and consequent structure collapse.

## 2. Materials and methods

### 2.1. Computer-aided designs

The different geometries, our objects of study, are designed with the help of Solid Edge (Siemens PLM Solutions), firstly by obtaining different unit cells and subsequently by using Boolean operations and two-dimensional or three-dimensional matrix replication. In most cases unit cells were repeated four times for the planar geometries and three times for the three-dimensional ones, in the different directions, for obtaining adequate auxetic behavior without increasing file size unnecessarily. Such repetitions were oriented at providing a more exact visual impression of the aspect of the auxetic structure, as sometimes if using just one unit cell it might not be so easy to imagine the final aspect. The planar auxetics are designed in the  $ZY$  plane for subsequent extrusion along the  $x$  direction, so the expected auxetic behavior leads to transversal contractions along the  $y$  axis, when compressed along the  $z$  direction. The three-dimensional auxetics are designed to investigate transversal contractions along  $x$  and  $y$  axes, when compressed along the  $z$  direction. In a similar way, tractions along the  $z$  direction lead to transversal expansions. A homogeneous thickness of 1.2 mm is used for the smaller features of the structures obtained, for promoting a more adequate comparison, especially in terms of equivalent Young’s modulus. Such a value of 1.2 mm corresponds to a wall thickness in the 2D structures and to a cross-section diameter in most 3D structures, with the exception of the ‘re-entrant cuboid’ structure for which such a value is given to wall thickness. We have tried to obtain structures with similar overall dimensions, with  $a \approx b \approx c$  for the 3D auxetics, and  $a \approx b/10 \approx c/10$  for the 2D auxetics, although some differences appear due to the use of cell units with different degree of complexity (see table 1).

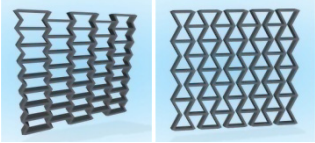
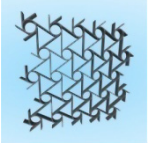
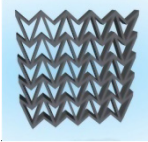
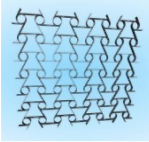
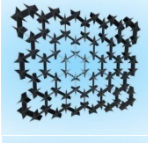
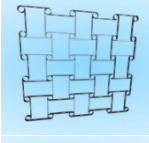
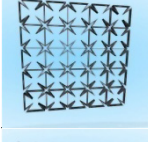
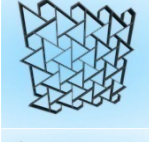
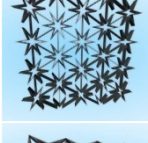
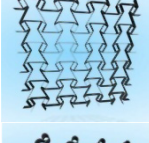
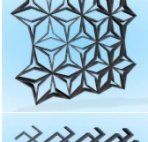
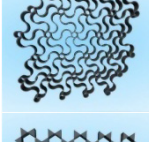
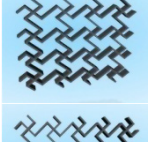
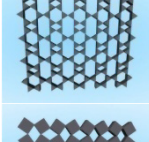
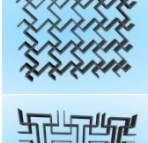
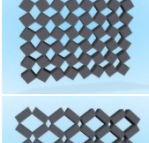
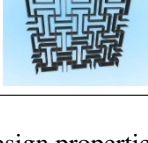
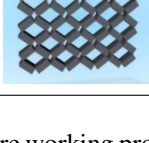
### 2.2. Finite-element method simulations

The different geometries are simulated using the finite-element method capabilities of NX-8.0 (Siemens PLM Solutions) for validating (or rejecting) their auxetic behavior

Q.3

Q.4

**Table 1.** Summary of planar auxetic (and potentially auxetic) geometries under study.

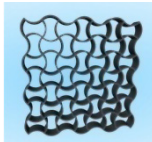
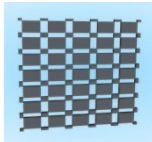


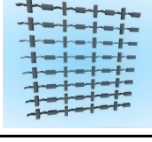
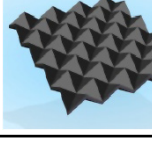
Geometry	CAD model	Geometry	CAD model
Re-entrant Masters–Evans (two models) [9–12, 22]		Chiral circular [16]	
Re-entrant triangular [13]		Chiral circular symmetric [16]	
Re-entrant star 3-n [11]		Chiral square symmetric [16]	
Re-entrant star 4-n [11]		Chiral hexagonal [16]	
Re-entrant star 6-n [11]		Chiral rectangular symmetric [16]	
Re-entrant hexagonal honeycomb [4]		Rotachiral [16]	
Lozenge grid oblong [14]		Rotating unit triangles [17]	
Lozenge grid square [14]		Rotating unit squares [17]	
Square grid [4]		Rotating unit rectangles v1 inspired by [17]	

and obtaining the values of relevant design properties. Details regarding material, mesh, loads, boundary conditions, solver parameters used, post-processing and results analysis are described along these lines. If adequate loads and boundary conditions are used, simulating using just a single unit cell is enough and speeds up the whole simulation process. However, in our case, as we had already designed the auxetic structures with repeated unit cells, we carried out the simulations using such CAD files, instead of just single unit cells. In any case, for us it was an adequate approach, as we were not so limited by computing resources or simulation time, and simulating a bigger structure let us assess more easily if the loads and

boundary conditions applied were working properly, verifying symmetry and global behavior.

**2.2.1. Material and mesh.** Tetrahedral ten-node elements are used for meshing, which is carried out with the help of the automatic meshing and refining tool from the software employed, which provides elements with sizes below 0.5 mm in almost all cases. Additionally more than 85% of the elements obtained had a skewness value lower than 0,7, which provides adequate meshes for the purposes of the present study. Epoxy resin has been selected as material for the simulations, as it is a material normally used in additive ‘layer

Table 1. (Continued.)

Geometry	CAD model	Geometry	CAD model
Re-entrant sinusoidal [4]		Rotating unit rectangles v2 inspired by [17]	
Microporous [4]		Clegg and Vandeperre [17]	
Liquid crystalline [15]		Egg rack mechanism [17, 18]	

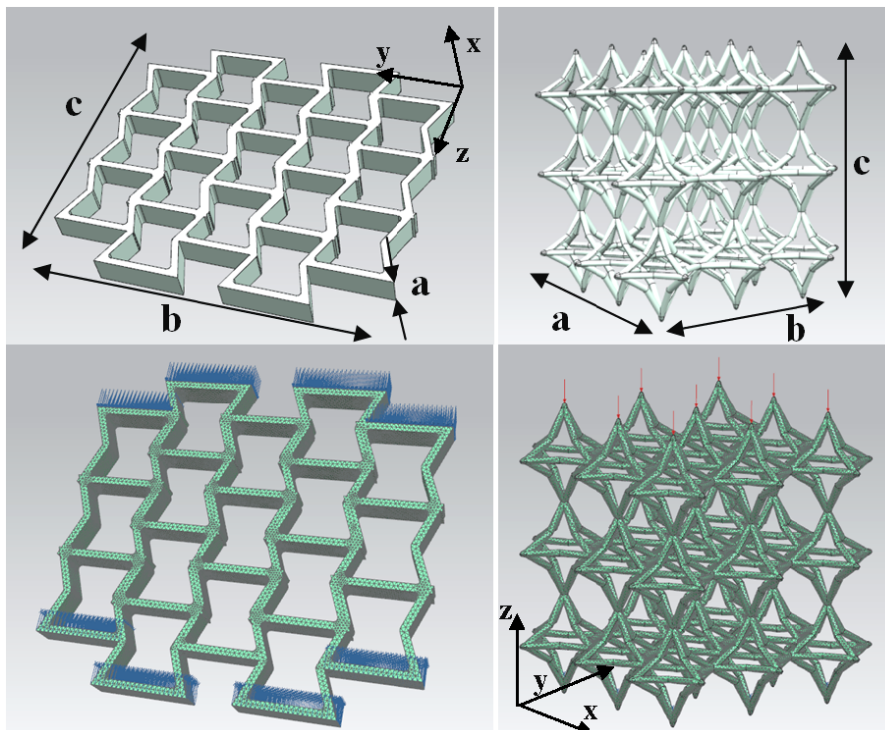


**Figure 1.** Upper images: example of overall dimensions  $a$ ,  $b$ ,  $c$  (related respectively to Cartesian directions  $x$ ,  $y$ ,  $z$ ) for planar (left column) and three-dimensional (right column) potentially auxetic structures. Lower images: example of loads and boundary conditions applied. Fixed displacements in the basis along direction ' $z$ ', leaving ' $x$ ' and ' $y$ ' directions unrestricted, and a group of punctual/distributed forces along direction ' $-z$ ' on upper face edges/faces for each structure under study.

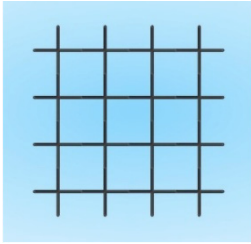
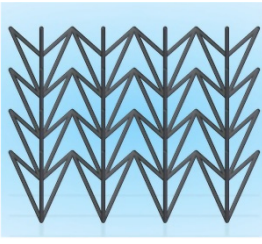
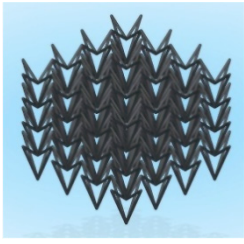
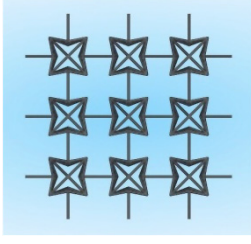
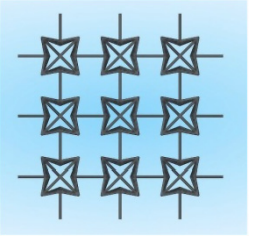
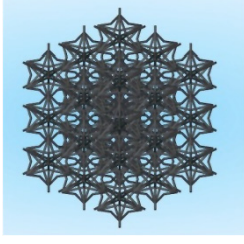
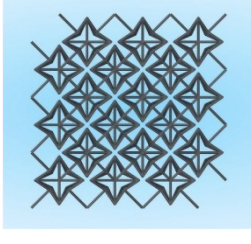
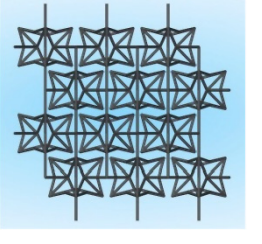
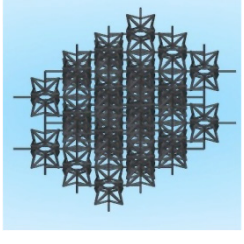
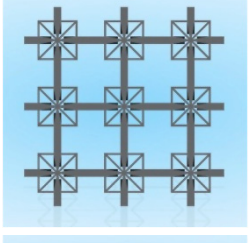
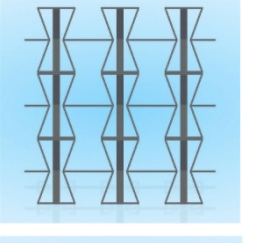
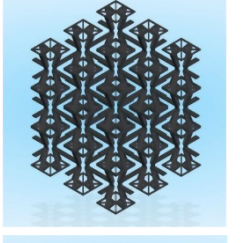
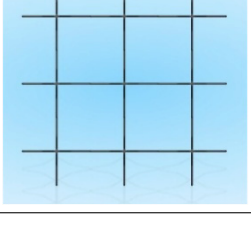
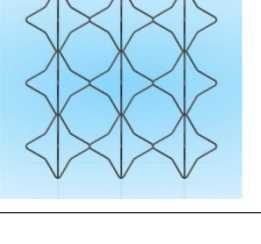
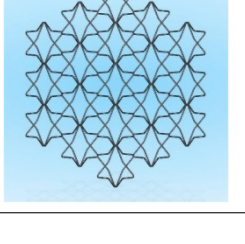
by layer' manufacturing technologies, which are normally used for obtaining physical prototypes of complex geometries with inner details, including auxetic models. Material bulk properties include a density of  $1300 \text{ kg m}^{-3}$ , a Young's modulus of  $3000 \text{ MPa}$ , a Poisson ratio of  $0.37$  and a yield strength of  $27 \text{ MPa}$ .

**2.2.2. Loads and boundary conditions.** As the load values for promoting relevant strains and subsequent adequate Poisson ratio measurements are initially unknown for the

different geometries, repetitive load cases with increasing values are used. Limit values are those that promote the beginning of contacts between inner features of the structures, when stress values start to increase also dramatically, even above yield strength, thus promoting structure collapse if higher values are applied.

Such limit cases help us also to obtain the maximum area or volume reduction attainable by each of the structures considered here, which is indeed useful for design tasks linked to expandable actuators and morphing structures. Nevertheless, previous recent research has also considered the

**Table 2.** Summary of three-dimensional auxetic (and potentially auxetic) geometries under study.

Model	Top view	Front view	Isometric view
Pyramid US Patent [19]			
Re-entrant idealized v1 [9]			
Re-entrant idealized v2 [9]			
Re-entrant cuboid Novel design			
Re-entrant octahedron v1 [20]			

possibility of using self-contact for promoting stress-relief [9], which should be further studied as discussed in section 3.4, even though the structures assessed here do not benefit from such a possibility.

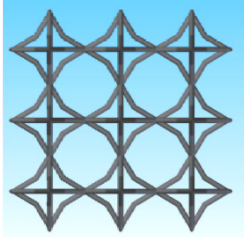
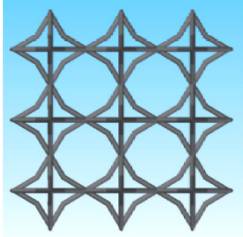
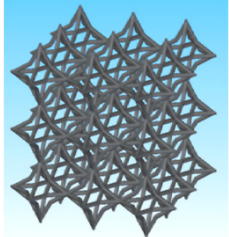
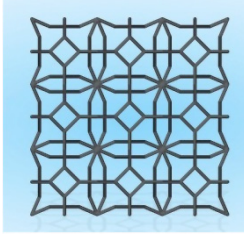
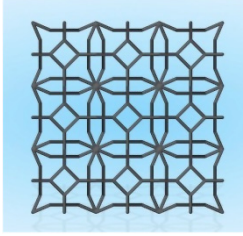
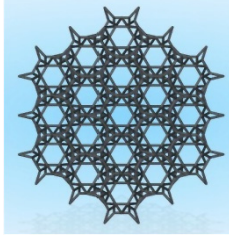
Loads are applied as a group of punctual forces along the  $-z$  direction on the upper face edges of the different structures, trying to promote symmetry and homogeneous loading, or as distributed forces when there are planar faces available. As boundary conditions, the vertical displacements of the lower face edges of the different structures are fixed. Displacements along  $x$  and  $y$  directions are free, so that auxetic behavior can be assessed in ideal conditions. In some cases a lower corner of the structure had to be fixed in all directions,

to avoid singularities during computing, but without actual influence on the properties under study.

Figure 1 includes some images of 2D and 3D potentially auxetic structures for providing some additional details about overall dimensions  $a, b, c$  (related to directions  $x, y, z$ ), as well as visual support regarding the different loads and boundary conditions applied for assessing the behavior of the different geometries—structures under study.

*2.2.3. Solver parameters and post-processing.* From the different possibilities of NX-8.0 for carrying out FEM simulations, NX-Nastran solver and structural analysis type (solution type SESTATIC 101) are selected with the option of

Table 2. (Continued.)

Model	Top view	Front view	Isometric view
Re-entrant octahedron v2 [20]			
Re-entrant tetracaidecahedron [21]			

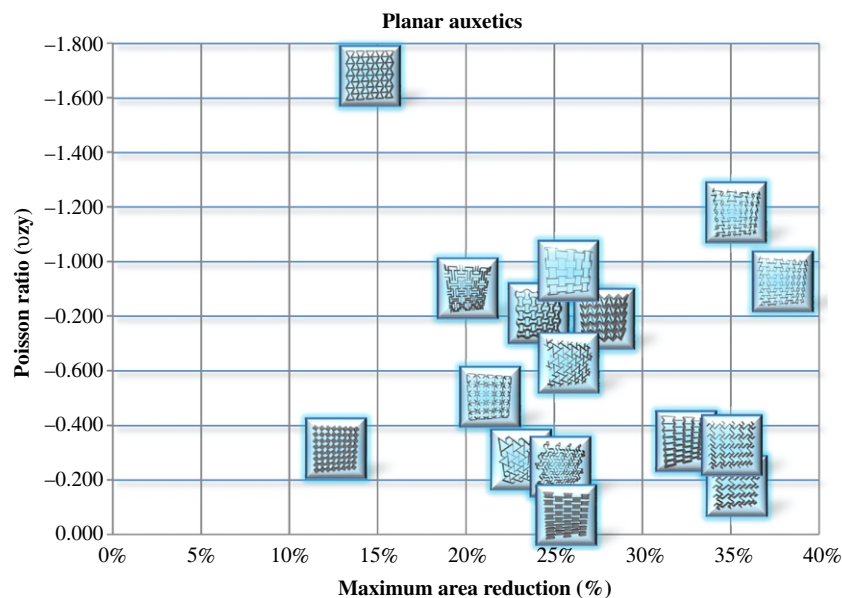


Figure 2. Summary of planar auxetics considering Poisson ratio and maximum area reduction.

‘element iterative solver’ activated as 3D elements are used for the simulations. Simulations are carried out at a default ambient temperature of 25 °C. It is important to remark the compatibility between the design and simulation programs, as geometries can be directly imported for simulation, without the typical limitations of universal format (.igs, .stl, .stp, ...) conversions and the information loss they normally involve. Once the simulations are carried out, post-processing tools allow for an easy measurement of displacements in the different directions for subsequent calculation of the Poisson ratios, of the area or volume reduction, due to the auxetic behavior during uniaxial compressions, and of the equivalent Young’s modulus of the different structures. Details regarding the different designs obtained and the results

from the simulations developed are presented, summarized and discussed in section 3.

### 3. Results and discussion

#### 3.1. CAD library of auxetic geometries

The library of auxetic and potentially auxetic geometries under study is summarized in tables 1 and 2, showing respectively the different CAD models of the planar and three-dimensional structures designed. Most of these geometries and names are selected from previous research, publications, patents and websites, and some of them include relevant adaptations or are even our own novel designs. In some cases a similar concept has been widely explored

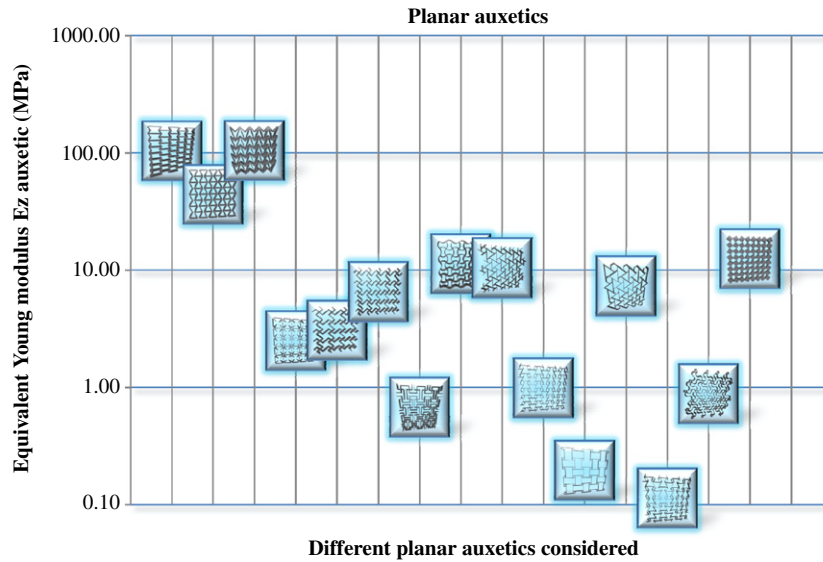


Figure 3. Summary of planar auxetics considering equivalent Young’s modulus.

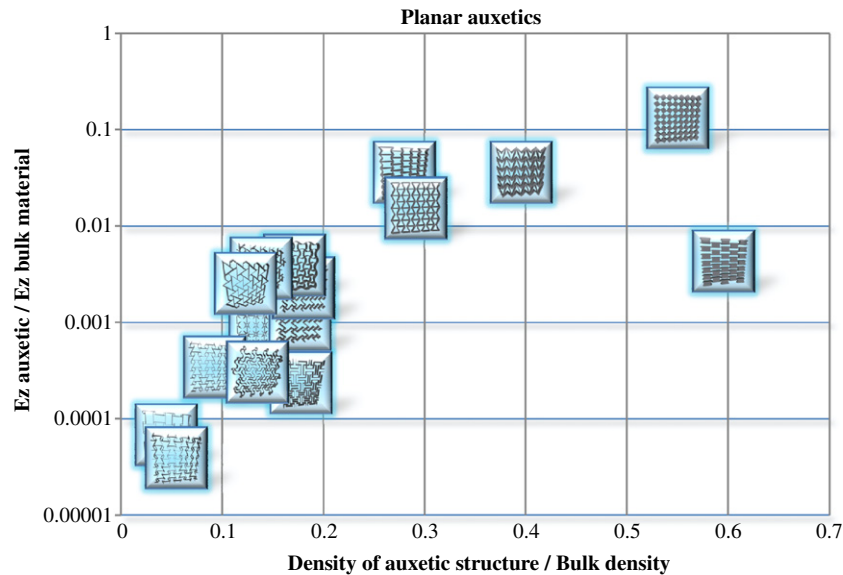


Figure 4. Normalized Young’s modulus versus normalized density of planar auxetics.

and different variations are included, as happens with the ‘Masters–Evans’, ‘re-entrant star’, ‘rotating units’ and ‘3D re-entrant’ geometries. Our intention is to make the library available online through our university website or by developing a collaborative site for download of the different geometries in .par format (Solid Edge) and other universal formats such as .stl for prototyping purposes, as well as for continuously updating and expanding the library.

### 3.2. Comparative study of the planar auxetics

From the 25 planar structures, a total of 20 are simulated for obtaining detailed information regarding Poisson ratio, maximum area reduction and equivalent Young’s modulus. Figures 2 and 3 represent the results from the simulations, showing respectively the values of ‘Poisson ratio’ versus

‘maximum area reduction’ and ‘equivalent Young’s modulus for different structures’ for those geometries whose actual auxetic behavior has been validated. It is important to note that only 16 of them provided auxetic behavior, as the ‘re-entrant star 6-n’, ‘re-entrant hexagonal honeycomb’, ‘rotating unit rectangles v1’ and ‘Clegg and Vandeperre’ expand laterally when vertically compressed, according to our simulations. A logarithmic scale has been used for the vertical axis of figure 3, for providing an easier to use comparative graphic. The ‘re-entrant star 3n’, ‘liquid crystalline’, ‘rotating unit triangles’ and ‘rotating unit rectangles v2’ proved to have too complex features for an adequate simulation and results could not be obtained. In the case of the ‘egg rack mechanism’ geometry, very important out-of-plane strains are obtained and additional restrictions are needed to promote auxetic behavior.

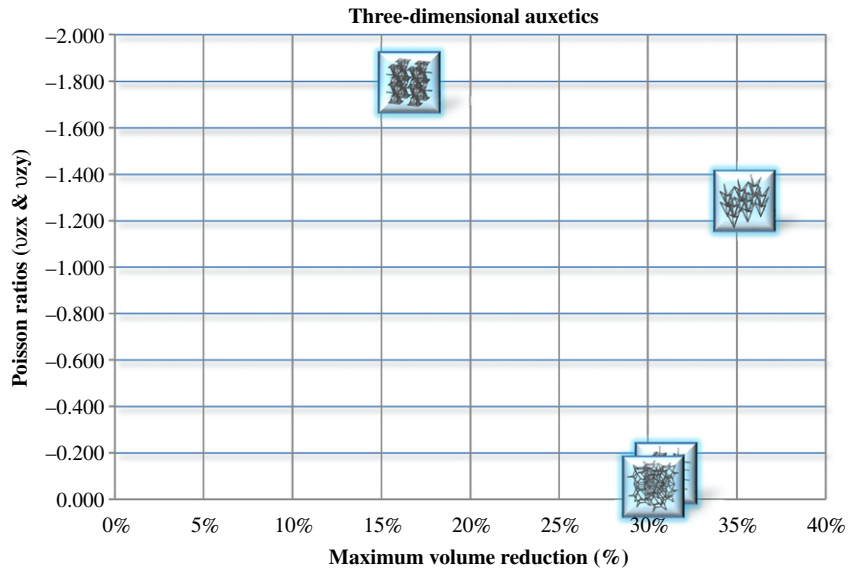


Figure 5. Summary of 3D auxetics considering Poisson ratio and maximum volume reduction.

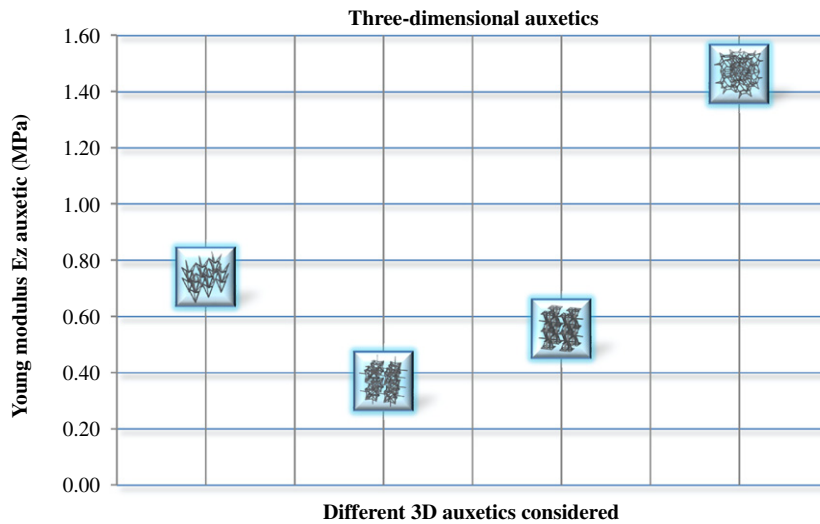


Figure 6. Summary of 3D auxetics considering equivalent Young’s modulus.

Figure 4 provides a performance map, relevant for using these kinds of geometries, not only for developing deployable systems, but also for their potential use as structural elements. The values of Young’s modulus ( $E_{z \text{ auxetic}}$ ) and density ( $\rho_{\text{auxetic}}$ ) of the planar auxetic structures have been normalized, dividing them by the values of Young’s modulus ( $E_{z \text{ bulk}}$ ) and density ( $\rho_{\text{bulk}}$ ) of the bulk material. A logarithmic scale has been used for the vertical axis of figure 4.

### 3.3. Comparative study of the three-dimensional auxetics

From the seven three-dimensional structures, a total of six are simulated for obtaining detailed information regarding Poisson ratios, maximum volume reduction and equivalent Young’s modulus. Figures 5 and 6 represent the results from the simulations, showing respectively the values of ‘Poisson ratios’ versus ‘maximum area reduction’ and ‘equivalent

Young’s modulus for different structures’ for those geometries whose actual auxetic behavior has been validated. It is important to note that only four of them provided auxetic behavior, as the ‘re-entrant octahedron v1’ and ‘re-entrant octahedron v2’ expand laterally when vertically compressed, according to our simulations.

Figure 7 provides an additional performance map, relevant for using these kinds of geometries as structural elements. The values of Young’s modulus ( $E_{z \text{ auxetic}}$ ) and density ( $\rho_{\text{auxetic}}$ ) of the three-dimensional auxetic structures have been normalized, dividing them by the values of Young’s modulus ( $E_{z \text{ bulk}}$ ) and density ( $\rho_{\text{bulk}}$ ) of the bulk material.

### 3.4. Final summary and discussion

A summary of simulation results, with the relevant design properties assessed, both for the planar and for the three-



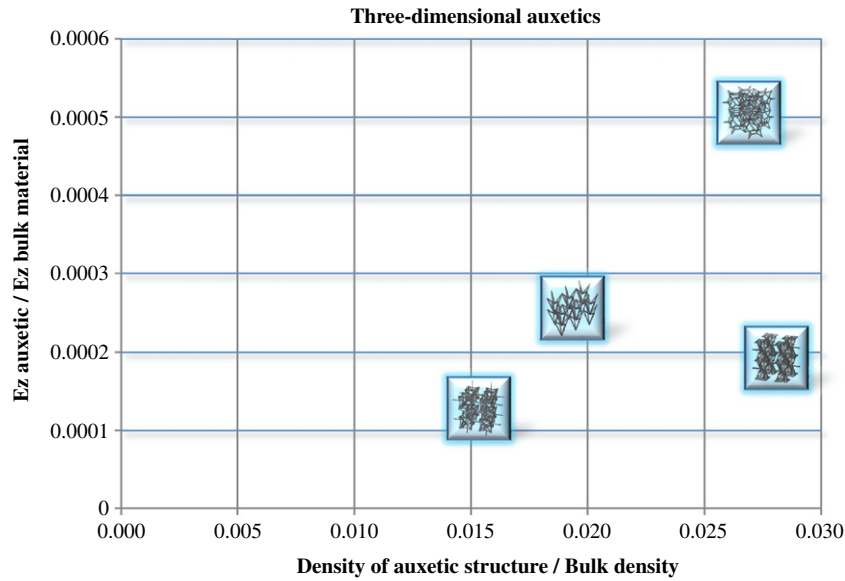


Figure 7. Normalized Young's modulus versus normalized density of 3D auxetics.

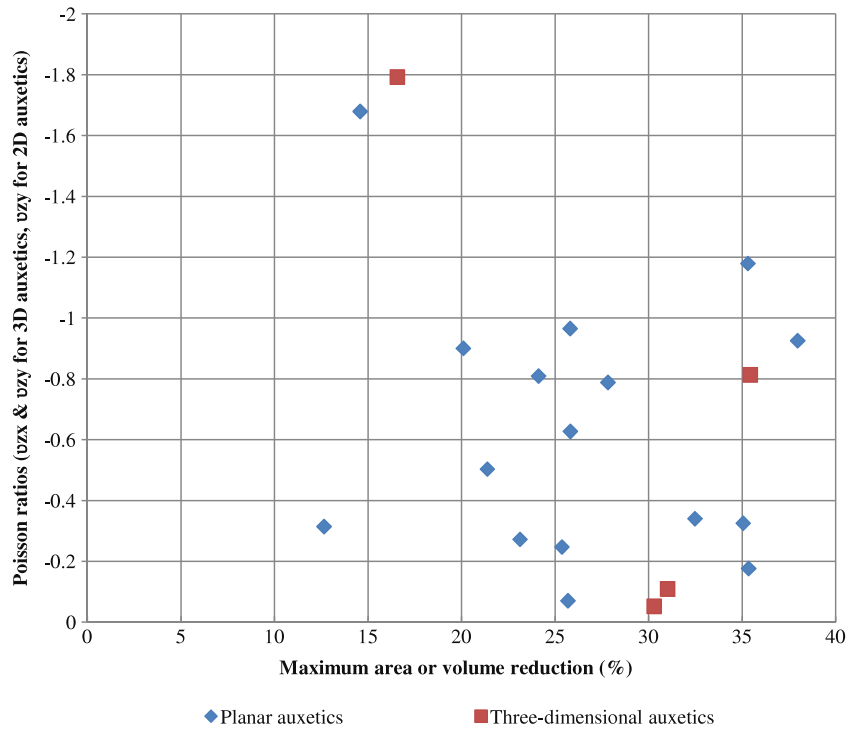


Figure 8. Relationship between Poisson ratio and maximum area or volume reduction for the different planar and three-dimensional auxetic geometries under study.

dimensional structures under study, is included in table 3 (together with some results from other auxetic materials) and shown graphically in figure 8. In this case data from those whose auxetic behavior has been validated and from those whose auxetic properties have been rejected, are taken into account for table 3, as they may be helpful for additional design tasks linked to devices based on such structures. Although from these results (see table 3 and figures 2–8) it is difficult to establish general trends and connections between

the different properties of auxetic geometries, it is important to remark some highly interesting details.

For the planar structures only the Poisson ratio  $\nu_{zy}$  is presented, as  $\nu_{zx} \approx 0$  due to a lack of relevant out-of-plane strains. For the three-dimensional structures the values  $\nu_{zy}$  and  $\nu_{zx}$  are always equal in these models, as they are obtained by means of Boolean operations starting from a unit cell, hence being symmetry promoted. Negative values of Poisson ratios up to  $-1,7$  or  $-1,8$  are obtained, both using planar and three-dimensional structures, although the most typical

Q.6

**Table 3.** Summary of properties assessed for the different auxetic geometries under study and for some materials previously reported with auxetic properties.

Planar structures			
Geometry	Poisson ratio ( $\nu_{zy}$ )	Maximum area reduction (%)	Equivalent Young's modulus (MPa)
Re-entrant Masters–Evans v1	−0.341	32.48	103.98
Re-entrant Masters–Evans v2	−1.68	14.58	44
Re-entrant triangular	−0.789	27.83	104
Re-entrant star 4-n	−0.504	21.38	2.51
Re-entrant star 6-n	0.152	NA	NA
Re-entrant hexagonal honeycomb	0.875	NA	NA
Lozenge grid oblong	−0.177	35.35	3.06
Lozenge grid square	−0.326	35.06	6.53
Square grid	−0.901	20.1	0.68
Re-entrant sinusoidal	−0.81	24.12	11.33
Microporous	−0.071	25.69	12.44
Chiral circular	−0.628	25.82	10.48
Chiral circular symmetric	−0.926	37.97	0.99
Chiral square symmetric	−0.966	25.81	0.2
Chiral hexagonal	−0.273	23.13	7.32
Chiral rectangular symmetric	−1.18	35.31	0.11
Rotachiral	−0.248	25.37	0.88
Rotating unit squares	−0.315	12.65	379.73
Rotating unit rectangles v1	0.69	NA	NA
Clegg and Vandepierre	0.142	NA	NA
Three-dimensional structures			
Geometry	Poisson ratios ( $\nu_{zy} \approx \nu_{zx}$ )	Maximum volume reduction (%)	Equivalent Young's modulus (MPa)
Pyramid US Patent	−0.814	35.44	0.74
Re-entrant idealized v1	−0.11	31.02	0.37
Re-entrant cuboid	−1.793	16.57	0.56
Re-entrant octahedron v1	0.997	NA	NA
Re-entrant octahedron v2	0.433	NA	NA
Re-entrant tetracaidecahedron	−0.053	30.3	1.46
Auxetic materials previously reported			
Material	Poisson ratios	Maximum volume reduction (%)	Equivalent Young's modulus (MPa)
Shape-memory polymer foam [27]	$\nu_{yx} = -0.95$ $\nu_{zx} \approx 0$	$\approx 80$	—
Shape-memory polymer auxetic foam [7]	$\nu_{zr1} \approx -0.17$ $\nu_{zr2} \approx -0.2$	$\approx 30$	—
Shape-memory alloy auxetic actuator [6]	$\nu_{zx} \approx -1$ $\nu_{zy} \approx -1$	$\approx 10-15$	—

values range from  $-0.1$  to  $-0.9$ . Those geometries with the most negative Poisson ratios ('re-entrant Masters–Evans v2' and 're-entrant cuboid') provide a maximum area or volume reduction around 15%, a typically low value, when compared with the most frequent 25%–40% range.

Regarding the values of equivalent Young's modulus, we would like to remark that auxetics, due to their lattice and light structures, are much more flexible than the bulk

material used for their manufacture; in this case with values in the range 1–5 MPa, although it can be easily modified and tuned to desired values by changing the thicknesses of the different features and the geometries of unit cells. It is also relevant to note that geometrical changes or adaptations of a basic structure have an influence on final properties, as can be seen when considering the differences between the 're-entrant Masters–Evans v1' and the 're-entrant

Masters–Evans v2', between the 'rotating unit squares' and the 'rotating unit rectangles' or between the 'Lozenge grid oblong' and 'Lozenge grid square', as preliminary comparisons for forthcoming more systematic analyses of the effect of geometrical changes on each of the auxetic designs have provided. In fact the influence of such geometrical changes or adaptations of a basic structure, for modifying the value of Poisson ratio obtained, has already been the subject of systematic research for some of the structure types here reviewed [23–25, 15].

In our study we have focused on providing a library of different types of auxetic geometries (re-entrant, chiral, rotating, . . . , both planar and three-dimensional) and assessing their typical values of Poisson coefficient, equivalent Young's modulus, equivalent density and maximum area or volume reduction, also trying to find some typically described 'auxetic' geometries, whose response is actually not auxetic. The values provided for the different properties can be conceived as an initial assessment for each of the designs reviewed, for helping in metamaterial selection tasks. Once a design is selected for its relationship between Poisson ratio, equivalent Young's modulus, equivalent density and maximum area or volume reduction, the specific effects of geometrical changes should be addressed, in case final property adaptation for a concrete application is needed.

Novel interesting designs, based on modifications upon some auxetics reviews here, take advantage from self-contact during compression, as a way for promoting stress-relief and achieving further area or volume reductions [26, 9]. Although the structures analyzed here do not benefit from stress-relief (and our consideration of the self-contact as a limiting value thus has some exceptions), it would hopefully be possible to obtain modifications from the designs included in the present library for promoting such a possibility. The adaptation of the 'Masters–Evans' structure presented by Mehta, Frecker and Lesieutre can be a source of inspiration for realizing similar design changes in other planar and three-dimensional auxetic structures. Regarding future directions it would also be interesting to provide an additional review focused on auxetics with stress-relief capabilities, hence helping to progressively improve the present CAD library of auxetic geometries.

In any case it is relevant to mention that, when these *ad hoc* designed auxetic geometries are compared with foam materials and other actuators previously reported as auxetics [27, 7, 6], several geometries assessed in this study provide more negative Poisson ratios, as well as a more remarkable symmetry, even though volume reductions cannot match some values reported for polymeric foams. Anyway this additional comparison is interesting and it would be also motivating to obtain CAD models mimicking foam-like auxetics for completing the developed library, possibly by using medical imaging technologies, together with MIMICS-like (materialize NV) software for converting such complex geometries into CAD files.

#### 4. Conclusions

A total of 32 potentially auxetic geometries have been designed, from which 26 have been simulated using

the finite-element method for obtaining relevant design properties, including Poisson ratio, maximum area or volume reduction and equivalent Young's modulus. The results from the simulations have helped to validate the auxetic behavior of 20 geometries and to detect six geometries typically cited as auxetic, but whose auxetic behavior is actually prevented due to lateral expansion, buckling and structure collapse. The library of auxetic geometries and the information provided may be of use for the development of novel actuators, structures and devices based on these interesting properties. The non-auxetic geometries can nonetheless be useful for developing morphing or foldable structures, even though such folding cannot be obtained by uniaxial loading and additional boundary conditions are needed.

#### Acknowledgments

We acknowledge reviewers for their positive comments and proposals for improvement, which have helped to provide a more detailed and clear explanation, as well as to complete the comparative study presented and to propose future directions.

#### References

- [1] Lakes R S 1987 Foam structures with a negative Poisson's ratio *Science* **235** 1038–40
- [2] Evans K E 1991 Auxetic polymers: a new range of materials *Endeavour* **15** 170–4
- [3] He C, Liu P, McMullan P J and Griffin A C 2005 Toward molecular auxetics: main chain liquid crystalline polymers consisting of laterally attached para-quaterphenyls *Phys. Status Solidi b* **242** 576–84
- [4] Liu Y and Hu H 2010 A review on auxetic structures and polymeric materials *Sci. Res. Essays* **5** 1052–63
- [5] Griffin A C, Kumar S and Mc Mullan P J 2005 Textile fibers engineered from molecular auxetic polymers *National Textile Center Research Briefs—Materials Competency* pp 1–2
- [6] Scarpa F, Jacobs S, Coconnier C, Toso M and Di Maio D 2010 Auxetic shape memory alloy cellular structures for deployable satellite antennas: design, manufacture and testing *EPJ Web of Conf.* **6** 27001
- [7] Bianchi M, Scarpa F and Smith C W 2010 Shape memory behaviour in auxetic foams: mechanical properties *Acta Mater.* **58** 858–65
- [8] Tan T W, Douglas G R, Bond T and Phani A S 2011 Compliance and longitudinal strain of cardiovascular stents: influence of cell geometry *J. Med. Dev.* **5** 041002
- [9] Mehta V, Frecker M and Leiseutre G A 2009 Stress relief in contact aided compliant cellular mechanisms *ASME J. Mech. Des.* **131** 091009
- [10] Goldstein R V, Gorodtsov V A and Lisovenko D S 2010 Anomalous elastic behaviour of micro and nanowhiskers with a cubic atomic structure *Ishlinsky Institute for Problems in Mechanics RAS—Teaching material*
- [11] Wei H and Wu G 2004 An approximation method for simulating temperature dependence of Poisson's ratios of self-expanding auxogens *Comput. Methods Sci. Technol.* **10** 1–6
- [12] Grima J, Gatt R, Alderson A and Evans K 2005 On the potential of connected stars as auxetic systems *Mol. Simul.* **31** 925–35

Q.7

Q.8

Q.9

- [13] Ugbolue S C, Kim Y K, Warner S B, Fan Q, Yang C L and Kyzymchuk O 2011 Auxetic fabric structures and related fabrication methods *US Patent Specification* 2011/0046715 A1
- [14] Larsen U D, Sigmund O and Bouwstra S 1997 Design and fabrication of compliant micromechanisms and structures with negative Poisson's ratio *J. Microelectromech. Syst.* **6** 99–107
- [15] Smith C W, Grima J N and Evans K E 2010 A novel mechanism for generating auxetic behaviour in reticulated foams: missing rib foam model *Acta Mater.* **48** 4349–56
- [16] Moratti S and Aldred P 2005 Dynamic simulations of potentially auxetic liquid-crystalline polymers incorporating swivelling mesogens *Mol. Simul.* **31** 883–7
- [17] Dirrenberger J, Forest S, Jeulin D and Colin C 2011 Homogenization of periodic auxetic materials *Proc. Eng.* **10** 1847–52
- [18] Grima J N 2011 Auxetic metamaterials [www.auxetic.info](http://www.auxetic.info) (last access: June 5th 2012)
- [19] Grima J N, Ravirala N, Galea R, Ellul B, Attard D, Gatt R, Alderson A, Rasburn J and Evans K E 2010 Modelling and testing of a foldable macrostructure exhibiting auxetic behavior *Phys. Status Solidi* **248** 117–22
- [20] Ma Z D 2011 Three-dimensional auxetic structures and applications thereof *US Patent Specification* 7910193 B2
- [21] Palz N 2009 Parametrically driven auxetic foam [www.grasshopper3d.com](http://www.grasshopper3d.com) (last access: June 5th 2012)
- [22] Friis E A, Lakes R S and Park J B 1988 Negative Poisson's ratio polymeric and metallic materials *J. Mater. Sci.* **23** 4406–14
- [23] Masters I G and Evans K E 1996 Models for the elastic deformation of honeycombs *Compos. Struct.* **35** 403–22
- [24] Xu B, Arias F, Brittain S T, Zhao X M, Grzybowski S T and Whitesides G M 1999 Making negative Poisson's ratio microstructures by soft lithography *Adv. Mater.* **11** 1186–9
- [25] Smith C W, Grima J N and Evans K E 2000 A novel method for generating auxetic behavior in reticulated foams: the missing rib foam method *Acta Mater.* **17** 4349–56
- [26] Mehta V, Frecker M and Lesieutre G 2008 Contact aided compliant mechanisms for morphing aircraft skin *Proc. SPIE 15th Int. Symp. on Smart Structures and Materials* vol 6296, pp 1–12
- [27] Maitland D J, Small I V W, Ortega J M, Buckley P R, Rodriguez J, Hartman J and Wilson T S 2007 Prototype laser-activated shape memory polymer foam device for embolic treatment of aneurysms *J. Biomed. Opt.* **12** 030504

## Queries for IOP paper 429872

*Journal:* SMS  
*Author:* J C Álvarez Elipe and A Díaz Lantada  
*Short title:* Comparative study of auxetic geometries by means of computer-aided design and engineering

---

### Page 1

#### [Query 1:](#)

Author: Please check the author names and affiliations carefully.

---

### Page 1

#### [Query 2:](#)

Author: Please check [7] given here.

---

### Page 2

#### [Query 3:](#)

Author: Is sense of re-wording OK here?

---

### Page 2

#### [Query 4:](#)

Author: 1,2 mm is changed to 1.2 mm here and similar cases. Please check.

---

### Page 8

#### [Query 5:](#)

Author: 'simetric' changed to 'symmetric' and 'piramid' changed to 'pyramid' throughout. OK?

---

### Page 9

#### [Query 6:](#)

Author: Reference [22] has been changed to [27] in table 3. Please check.

---

### Page 11

#### [Query 7:](#)

Author: Please check the details for any journal references that do not have a blue link as they may contain some incorrect information. Pale purple links are used for references to arXiv e-prints.

---

### Page 11

#### [Query 8:](#)

Author: [2]: Year '2004' has been changed to '1991'. Please check.

---

### Page 11

#### [Query 9:](#)

Author: [10]: Please provide place and publisher.